

# Ab Initio Configuration Interaction Study of the Metal–Metal Coupling in Some Zr(III) and Ti(III) Dimers. Evidence for a “Superlong” Zr–Zr Bond in $[\text{Cp}_2\text{Zr}(\mu\text{-PR}_2)]_2$ and Related Complexes

Marc Bénard\* and Marie-Madeleine Rohmer

Contribution from the Laboratoire de Chimie Quantique, U.P.R. 139 du CNRS, Université Louis Pasteur, 4 rue B. Pascal, F-67000 Strasbourg, France. Received October 31, 1991

**Abstract:** The metal–metal distance in  $[\text{Cp}_2\text{Zr}(\mu\text{-PH}_2)]_2$  (**1**) and  $[\text{Cp}_2\text{Ti}(\mu\text{-Cl})]_2$  (**2**) has been optimized by means of ab initio configuration interaction (CI) calculations, all other distances being kept constant at their experimental values. The computed equilibrium distances are  $d_{\text{Zr-Zr}} = 3.77 \text{ \AA}$  and  $d_{\text{Ti-Ti}} = 3.965 \text{ \AA}$ , in good agreement with the observed structures. The singlet–triplet (S–T) splitting computed for **1** at the observed geometry is  $10065 \text{ cm}^{-1}$ . The computed S–T splitting of the Zr(III) dimer steadily decreases as the Zr–Zr distance increases, thus supporting the interpretation of the diamagnetism of **1** in terms of a through-space metal–metal coupling. In the hypothetical, unsupported Zr(III) dimer  $[\text{Cp}_2\text{Zr}]_2^{2+}$ , the S–T splitting is computed to be close to  $14000 \text{ cm}^{-1}$  at  $d_{\text{Zr-Zr}} = 3.65 \text{ \AA}$ , thus ruling out the hypothesis of a superexchange origin for the observed diamagnetism. The Zr–Zr distances of  $\sim 3.6 \text{ \AA}$  observed in  $[\text{Cp}_2\text{Zr}(\mu\text{-X})]_2$  dimers (X = I, PR<sub>2</sub>) should be interpreted as a compromise between the steric repulsion originating in the Cp rings and the restoring force associated with the metal–metal bond. The computed S–T splitting of the titanium dimer **2** appears much lower, due to the relatively weak 3d–3d overlap. Beyond 3.3–3.4 Å, the Ti–Ti interaction can be assimilated to an antiferromagnetic coupling, in agreement with the reported magnetic behavior of the  $[\text{Cp}_2\text{Ti}(\mu\text{-X})]_2$  complexes. The weakness of the Ti–Ti coupling explains why the metal–metal distances reported for those Ti(III) dimers are consistently longer than those reported for equivalent Zr(III) complexes. Direct metal–metal bonds can exist, however, in Ti(III) dimers lacking steric strain. The case of  $[\text{Cp}(\mu\text{-}\eta^1\text{:}\eta^5\text{-C}_5\text{H}_4)\text{Ti}(\text{PMe}_3)]_2$  ( $d_{\text{Ti-Ti}} = 3.223 \text{ \AA}$ ) has been investigated using ab initio CI calculations. The dimer is described in terms of two  $\text{Cp}_2\text{ML}_3$  fragments coupled by means of a bent metal–metal bond. In spite of the bond bending ( $\alpha = \sim 20^\circ$ ), the overlap of the metal hybrids is better than for  $[\text{Cp}_2\text{Ti}(\mu\text{-Cl})]_2$  at a similar Ti–Ti distance. The computed S–T splitting is  $4607 \text{ cm}^{-1}$ , accounting for the reported diamagnetism.

## 1. Introduction

About four years ago, no more than one edge-sharing bioctahedron containing Zr(III) atoms had been structurally characterized.<sup>1</sup> The development of new synthetic routes leading to two metal(III) d<sup>1</sup> fragments held together by a fulvalene ligand<sup>2</sup> has induced a growing interest in the structure<sup>3–5,7</sup> and reactivity<sup>6</sup> of the  $(\text{Zr}_2)^{6+}$  entity. The characterization of Zr(III)–Zr(III) distances ranging from 3.099 Å in  $\text{Zr}_2\text{Cl}_6(\text{dppe})_2^3$  to 3.669 Å in  $(\text{Cp}_2\text{ZrI})_2^{4b}$  has raised the question of the existence of a metal–metal coupling in those complexes.<sup>4–7</sup> It was generally considered that Zr–Zr distances over 3.4 Å were too long to be compatible with a metal–metal bond, but the consistent diamagnetism of all  $(\text{Zr}_2)^{6+}$  complexes remained puzzling. In a recent paper,<sup>8</sup> we suggested on the basis of extended Hückel and ab initio calculations that the Zr–Zr  $\sigma$  bond could persist at very long metal–metal distances, as a consequence of the unusually high polariz-

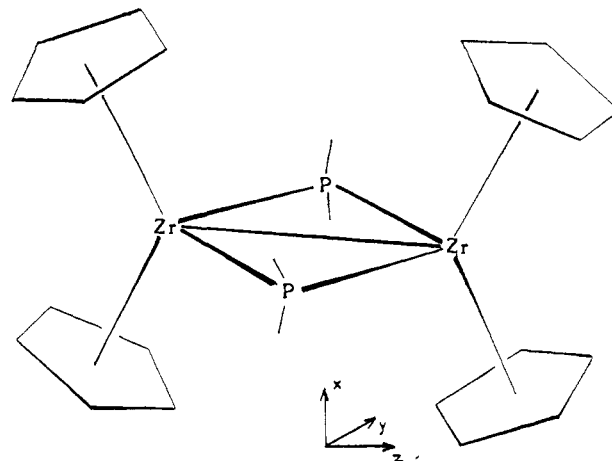


Figure 1. The  $[\text{Cp}_2\text{Zr}(\mu\text{-P}(\text{CH}_2)_2)]_2$  molecule.

(1) Wengrovius, J. H.; Schrock, R. R.; Day, C. S. *Inorg. Chem.* **1981**, *20*, 1844.

(2) (a) Asworth, T. V.; Cuenca, T.; Herdtweck, E.; Herrmann, W. A. *Angew. Chem.* **1986**, *98*, 278; *Angew. Chem., Int. Ed. Engl.* **1986**, *25*, 289. (b) Cuenca, T.; Herrmann, W. A.; Asworth, T. V. *Organometallics* **1986**, *5*, 2514. (c) Gambarotta, S.; Chiang, M. Y. *Ibid.* **1987**, *6*, 897. (d) Wielstra, Y.; Gambarotta, S.; Spek, A. L. *Ibid.* **1990**, *9*, 2142.

(3) Cotton, F. A.; Diebold, M. P.; Kibala, P. A. *Inorg. Chem.* **1988**, *27*, 799.

(4) (a) Chiang, M. Y.; Gambarotta, S.; van Bolhuis, S. *Organometallics* **1988**, *7*, 1864. (b) Wielstra, Y.; Gambarotta, S.; Meetsma, A.; de Boer, J. L. *Ibid.* **1989**, *8*, 250. (c) Wielstra, Y.; Gambarotta, S.; Meetsma, A.; Spek, A. L. *Ibid.* **1989**, *8*, 2948. (d) Wielstra, Y.; Gambarotta, S.; Spek, A. L.; Smeets, W. J. J. *Ibid.* **1990**, *9*, 2142. (e) Wielstra, Y.; Meetsma, A.; Gambarotta, S.; Khan, S. *Ibid.* **1990**, *9*, 876.

(5) (a) Ho, J.; Stephan, D. W. *Organometallics* **1991**, *10*, 3001. (b) Dick, D. G.; Stephan, D. W. *Can. J. Chem.* **1991**, *69*, 1146.

(6) (a) Herrmann, W. A.; Cuenca, T.; Menjon, B.; Herdtweck, E. *Angew. Chem.* **1987**, *99*, 687; *Angew. Chem., Int. Ed. Engl.* **1987**, *26*, 697. (b) Herrmann, W. A.; Menjon, B.; Herdtweck, E. *Organometallics* **1991**, *10*, 2134.

(7) Cotton, F. A.; Shang, M.; Wojtczak, W. A. *Inorg. Chem.* **1991**, *30*, 3670.

(8) Rohmer, M.-M.; Bénard, M. *Organometallics* **1991**, *10*, 157.

ability of the Zr(III) valence orbital. In parallel to that work, Herrmann et al.<sup>6</sup> investigated the reactivity of  $(\mu\text{-}\eta^5\text{:}\eta^5\text{-C}_{10}\text{H}_8)[(\mu\text{-Cl})\text{Zr}(\eta^5\text{-C}_5\text{H}_5)]_2$  with diphenyldiazomethane and *tert*-butyl isocyanide and concluded that the observed chemical behavior, typical of organozirconium chemistry, supports the existence of a metal–metal bond in the starting material.

The goal of the present paper is to assert the theoretical evidence for the existence of a metal–metal  $\sigma$  bond in the bridged  $\text{ZrCp}_2$  dimers and for the lack of such a bond in the equivalent complexes of titanium, taking as a criterion the singlet–triplet energy separation. Optimization of the metal–metal distance has been carried out at the CI level for real and model dimers of zirconium and titanium in order to ascertain the steric origin of the Zr–Zr bond stretching. Finally, we report and discuss the electronic structure of  $[\text{Cp}(\mu\text{-}\eta^1\text{:}\eta^5\text{-C}_5\text{H}_4)\text{Ti}(\text{PH}_3)]_2$ , in order to show that a metal–metal bond can also exist in Ti(III) dimers provided that the two moieties of the molecule are not pulled apart by ligand–ligand repulsion.

## 2. Computational Strategy

The metal-metal distances of  $[\text{Cp}_2\text{Zr}(\mu\text{-PH}_2)]_2$  (**1**) and  $[\text{Cp}_2\text{Ti}(\mu\text{-Cl})]_2$  (**2**) have been optimized at the ab initio configuration interaction (CI) level, starting from the structural characterization of the titanium dimer<sup>9</sup> and from that of  $[\text{Cp}_2\text{Zr}(\mu\text{-P}(\text{Me}_2))]_2$ <sup>4a</sup> (Figure 1). In the latter complex, the dimethylphosphido ligand was modeled into  $\text{PH}_2$  assuming a PH bond length of 1.42 Å. The metal-metal distance was then varied without modifying either the geometry of the  $\text{MCp}_2$  fragments or the distance between the metal and the bridging atoms.

We suggested in our previous report that the unusual length of the Zr-Zr bonds observed in  $[\text{Cp}_2\text{Zr}(\mu\text{-X})]_2$  ( $\text{X} = \text{I}, \text{PMe}_2$ ) and related complexes should be attributed to the steric repulsion induced by H...H contacts between the  $\text{ZrCp}_2$  moieties. In order to prove this hypothesis, we optimized the metal-metal distance in a model dimer of Zr(III) built from the same  $[\text{Zr}(\text{PH}_2)]_2$  core as **1** but free of steric repulsion. This hypothetical molecule was designed by replacing the four Cp rings by as many chlorine atoms located along the  $\text{Zr}-\Omega_{\text{Cp}}$  direction and assuming a Zr-Cl distance of 2.52 Å.<sup>10</sup> Although  $[\text{Cl}_2\text{Zr}(\mu\text{-PH}_2)]_2$  (**3**) has no chance of being isolated because of the highly unsaturated character of the metal, it provides a correct model for our distance optimization purpose, since (i) it retains electroneutrality and (ii) the change in the peripheral ligands has a negligible influence on the metal  $\sigma$  and  $\sigma^*$  frontier orbitals.

The singlet-triplet energy separation has been computed at all considered geometries of molecules **1**, **2**, and **3**, and that property has been used as a criterion for the presence or lack of a metal-metal  $\sigma$  bond. All considered molecules being bridged dimers, one may argue that even a large S-T splitting does not necessarily attest the presence of a metal-metal bond, since it might originate in a superexchange coupling involving the bridging ligands. In order to investigate this hypothesis, we computed the S-T splitting associated with a second model complex, now designed to retain the electronic configuration of **1**, in an unbridged structure. Since the optimization of the Zr-Zr distance was not planned for that complex, electroneutrality was not a prerequisite anymore. Then, the phosphido bridges were removed, and the oxidation state (III) of the metal was kept by considering the dication  $[\text{Cp}_2\text{Zr}]_2^{2+}$  (**4**). The geometry of the  $\text{ZrCp}_2$  moiety was kept as in **1**, and the Zr-Zr distance was fixed at 3.653 Å, that is, the bond length observed for  $[\text{Cp}_2\text{Zr}(\mu\text{-P}(\text{Me}_2))]_2$ <sup>4a</sup>. We finally consider the possibility for a direct Ti-Ti bond in  $[\text{Cp}(\mu\text{-}\eta^1\text{-}\eta^5\text{-C}_5\text{H}_4)\text{Ti}(\text{PMe}_3)]_2$  (**5**), a dimer of Ti(III) characterized by Kool et al.<sup>11</sup> A CI calculation is carried out using the experimental geometry ( $d_{\text{Ti-Ti}} = 3.22$  Å) and modeling the trimethylphosphine ligands by  $\text{PH}_3$  substituents.

The basis sets were designed as follows: for zirconium, we used a (15, 10, 9) basis set obtained by adding a p-type orbital (exponent 0.12) and a diffuse d orbital (exponent 0.045) to the standard set optimized by Veillard and Dedieu;<sup>12</sup> for titanium, a (13, 9, 6) basis set was taken from the (13, 7, 5) set of Hyla-Kryspin et al.<sup>13</sup> and improved with two functions (exponents 0.15 and 0.05) describing the 4p orbital and one d-type diffuse function (exponent 0.05). The contraction was [6, 4, 5] for Zr and [5, 4, 4] for Ti, corresponding to a quadruple- $\zeta$  description of the outer d shell. The basis set for phosphorus is (12, 8, 2) contracted into [5, 4, 2]. The basis sets for other atoms are (12, 8) contracted into [5, 4] for Cl; (9, 5) contracted into [3, 2] for C; and (4) contracted into [2] for H. Those basis sets were taken from Huzinaga<sup>14</sup> and

(9) Jungst, R.; Sekutowski, D.; Davis, J.; Luly, M.; Stucky, G. *Inorg. Chem.* **1977**, *16*, 1645.

(10) This value was taken from the characterization of zirconium complexes with terminal Cl ligands. See, for instance: (a) Erker, G. *Angew. Chem.* **1989**, *101*, 411; *Angew. Chem., Int. Ed. Engl.* **1989**, *28*, 397. (b) Erker, G.; Krüger, C.; Schlund, R. *Z. Naturforsch.* **1987**, *B42*, 1009. (c) Erker, G.; Schlund, R.; Krüger, C. *J. Organomet. Chem.* **1988**, *338*, C4. (d) Erker, G.; Schlund, R.; Krüger, C. *J. Chem. Soc., Chem. Commun.* **1986**, 1403.

(11) Kool, L. B.; Rausch, M. D.; Alt, H. G.; Herberhold, M.; Thewalt, U.; Honold, B. *J. Organomet. Chem.* **1986**, *310*, 27.

(12) Veillard, A.; Dedieu, A. *Theor. Chim. Acta* **1984**, *65*, 215.

(13) Hyla-Kryspin, I.; Demuyck, J.; Strich, A.; Bénard, M. *J. Chem. Phys.* **1981**, *75*, 3954.

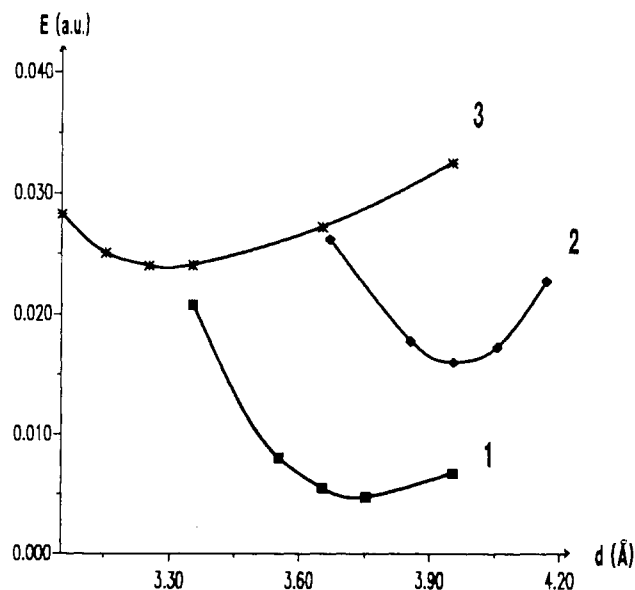


**Figure 2.** Potential energy curves (in hartrees) computed for  $[\text{Cp}_2\text{Zr}(\mu\text{-PH}_2)]_2$  (**1**),  $[\text{Cp}_2\text{Ti}(\mu\text{-Cl})]_2$  (**2**), and the model complex  $[\text{Cl}_2\text{Zr}(\mu\text{-PH}_2)]_2$  (**3**) as a function of the metal-metal distance. The Ti-Cl and Zr-P distances are kept fixed at their experimental values. The computed energies at equilibrium (hartrees) are -8515.2879 for **1**, -3379.9041 for **2**, and -9582.9407 for **3**.

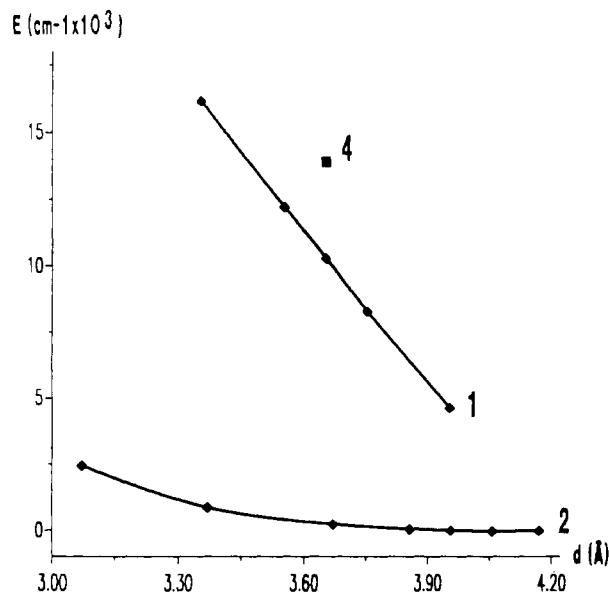


**Figure 3.** Singlet-triplet energy splitting ( $\text{cm}^{-1} \times 10^3$ ) computed for  $[\text{Cp}_2\text{Zr}(\mu\text{-PH}_2)]_2$  (**1**) and  $[\text{Cp}_2\text{Ti}(\mu\text{-Cl})]_2$  (**2**) as a function of the metal-metal distance. The Ti-Cl and Zr-P distances are kept fixed at their experimental values. The S-T splitting computed for  $(\text{Cp}_2\text{Zr})_2^{2+}$  (**4**) at  $d_{\text{Zr-Zr}} = 3.65$  Å is indicated.

modified as reported in ref 8, except for the basis set of phosphorus, which now includes two d functions with exponents 0.9 and 0.3. The SCF calculations were then carried out using the ASTERIX system of programs,<sup>15</sup> and the CI expansions were performed by using Siegbahn's contracted CI program.<sup>16</sup>

(14) (a) For the basis set of hydrogen: Huzinaga, S. *J. Chem. Phys.* **1965**, *42*, 1293. (b) For other atoms: Huzinaga, S. *Technical Report*, 1971; University of Alberta, Edmonton.

(15) (a) Ernenwein, R.; Rohmer, M.-M.; Bénard, M. *Comput. Phys. Commun.* **1990**, *58*, 305. (b) Rohmer, M.-M.; Demuyck, J.; Bénard, M.; Wiest, R.; Bachmann, C.; Henriot, C.; Ernenwein, R. *Ibid.* **1990**, *60*, 127. (c) Wiest, R.; Demuyck, J.; Bénard, M.; Rohmer, M.-M.; Ernenwein, R. *Ibid.* **1991**, *62*, 107. (d) Rohmer, M.-M.; Ernenwein, R.; Ulmschneider, M.; Wiest, R.; Bénard, M. *Int. J. Quantum Chem.* **1991**, *40*, 723.

(16) Siegbahn, P. E. M. *Int. J. Quantum Chem.* **1983**, *23*, 1869. The CI program was interfaced with ASTERIX by C. Daniel, M.-M. Rohmer, and M. Spéri.

The CI expansions leading to the energy of the lowest singlet and triplet states were carried out according to the two-step procedure detailed in ref 8. The first step, designed to optimize the frontier orbitals and more specifically the  $\sigma$  and  $\sigma^*$  metal orbitals, consists of a CI expansion carried out with respect to the  $\sigma^2\sigma^{*0}$  and  $\sigma^0\sigma^{*2}$  reference configurations, over a limited set of SCF valence orbitals, both occupied and virtual. The natural orbitals (NOs) deduced from the diagonalization of the first-order density matrix are expected to provide a good starting point for a balanced description of both the left-right and the dynamic correlation.<sup>17</sup> The strongly occupied NOs with a population less than 1.99 e and belonging to the same irreducible representations as the  $\sigma$  and  $\sigma^*$  orbitals are then retained for the final, multireference CI expansion. The corresponding electrons are then correlated with respect to the complete set of virtual orbitals belonging to the same representation as  $\sigma$  and  $\sigma^*$ .<sup>18</sup>

### 3. Results and Discussion

The potential energy curves and the singlet-triplet energy separation obtained at the CI level for **1**, **2**, and **3** are respectively displayed in Figures 2 and 3. The metal-metal distances characterized for  $[\text{Cp}_2\text{Zr}(\mu\text{-PMe}_2)_2]$  and  $[\text{Cp}_2\text{Ti}(\mu\text{-Cl})_2]$  are correctly reproduced by the calculations. The computed equilibrium positions correspond to M-M distances of 3.77 Å for the zirconium dimer (experimentally 3.653 Å<sup>4a</sup>) and 3.965 Å for the titanium complex (experimentally 3.943 and 3.968 Å for two independent molecules characterized in the crystallographic unit<sup>10</sup>). The potential well of the titanium dimer is relatively steep and symmetric compared to that of the dizirconium system. This should be attributed to the repulsion that develops in **2** between the bridging chlorine atoms when the metallacycle distorts toward larger Ti-Ti distances.

Replacing Cp ligands by chlorine atoms has a dramatic effect on the potential energy curve of the zirconium dimer. The metal-metal distance at equilibrium decreases from 3.77 to 3.30 Å. Since the frontier orbitals of the metallacycle, more specifically the  $\sigma_{\text{Zr-Zr}}$  (HOMO) and  $\sigma^*_{\text{Zr-Zr}}$  (LUMO), remain relatively unaffected by the change in the surrounding ligands, we expect the 0.47-Å variation of the metal-metal distance to account for the repulsive interactions that develop at short metal-metal distances between the four Cp rings.<sup>8</sup> In the hypothetical complex **3**, the energy variation is particularly smooth when the Zr-Zr distance increases beyond the equilibrium position ( $\sim 4.5$  kcal/mol<sup>-1</sup> between  $d_{\text{Zr-Zr}} = 3.3$  Å and  $d_{\text{Zr-Zr}} = 3.9$  Å, Figure 2). The shallowness of the potential curve explains the large displacement of the equilibrium position induced by steric crowding. The metal-metal distance computed for **3** is compatible with the Zr-Zr bond lengths characterized for dimers of Zr(III) in which the steric repulsion is expected either to vanish<sup>22</sup> or to be somewhat reduced as in some fulvalene derivatives.<sup>23</sup>

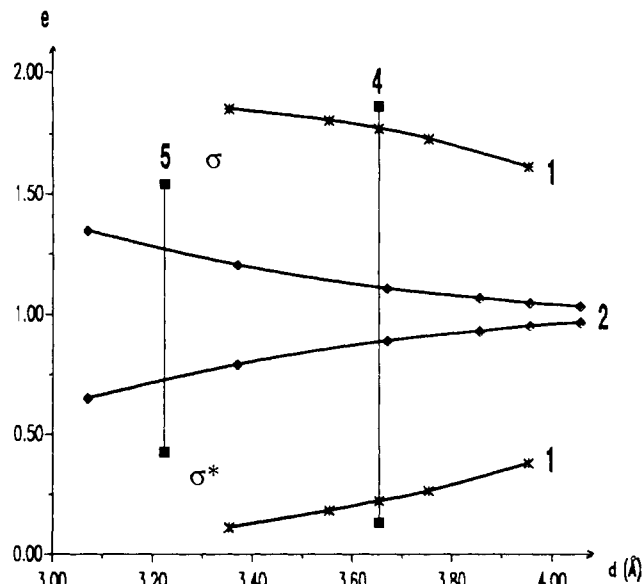


**Figure 4.** Population of the  $\sigma$  and  $\sigma^*$  natural orbitals for  $[\text{Cp}_2\text{Zr}(\mu\text{-PH}_2)_2]$  (**1**) and  $[\text{Cp}_2\text{Ti}(\mu\text{-Cl})_2]$  (**2**) as a function of the metal-metal distance. The populations obtained for  $(\text{Cp}_2\text{Zr})_2^{2+}$  (**4**) at  $d_{\text{Zr-Zr}} = 3.65$  Å and for  $[\text{Cp}(\mu\text{-}\eta^5\text{-C}_5\text{H}_4)\text{Ti}(\text{PMe}_3)_2]$  (**5**) ( $d_{\text{Ti-Ti}} = 3.223$  Å) are indicated.

The observed diamagnetism of the Zr(III) dimer had been attributed to the presence of a metal-metal single bond as long as the Zr-Zr distance did not exceed 3.3 Å.<sup>2a,3</sup> Strong antiferromagnetic coupling involving the bridging ligands had then been advocated when the longer metal-metal distances seemed hardly compatible with a through-space Zr-Zr interaction.<sup>4</sup> The present work shows, however, that the origin of the S-T splitting in the Zr(III) dimers and its evolution with the deformation of the metallacycle cannot be related to any kind of superexchange mechanism. The lowest triplet state obtained from the CI expansion originates almost exclusively (95–97%) in the  $\sigma^1\sigma^{*1}$  configuration in which the two singly occupied orbitals have nearly pure metal character. The S-T energy separation almost linearly decreases from 16 160 cm<sup>-1</sup> at  $d_{\text{Zr-Zr}} = 3.35$  Å to 4650 cm<sup>-1</sup> at  $d_{\text{Zr-Zr}} = 3.95$  Å, reflecting a slow but steady relocation of the two metal electrons as the Zr-Zr distance increases. This relocation is illustrated by the increasing population of the  $\sigma^*$  orbital in the ground-state singlet (Figure 4). Those results are compatible only with the existence of a direct metal-metal bond between strongly overlapping  $d_{z^2}$  orbitals. As can be expected, this overlap steadily diminishes when the metal-metal distance increases, and the unusual character of the overlapping atomic orbitals comes from their remarkable expansion in space. The zirconium  $\sigma$  orbital spans the whole set of four Gaussian functions describing the valence d shell, with notable contribution from each of them, including the most diffuse one. In order to definitely assess the through-space character of the metal-metal coupling, the S-T splitting has been computed for the hypothetical Zr(III) dimer  $(\text{Cp}_2\text{Zr})_2^{2+}$ , devoid of bridging ligands, at a Zr-Zr distance of 3.65 Å. Rather surprisingly, the computed splitting, 13 910 cm<sup>-1</sup>, is larger than in complex **1** at the same metal-metal distance (Figure 3). The origin of this unexpected increase of the S-T splitting should be traced to electronic effects that develop in the bridged dimers when the metallacycle is distorted toward large metal-metal distances. The bridging ligands are then approaching each other, and the contact of the  $\sigma$  lone pairs creates at the center of the cycle an area of nonbonding charge concentration. The contact of this charge concentration with the overlapping  $d_{z^2}$  metal

(17) (a) Löwdin, P. O. *Phys. Rev.* **1955**, *97*, 1474. (b) Bender, C. F.; Davidson, E. R. *Ibid.* **1969**, *183*, 23. (c) Schaefer, H. F., III. *J. Chem. Phys.* **1971**, *54*, 2207. (d) Caballol, R.; Malrieu, J.-P. *Chem. Phys.* **1990**, *140*, 7. (e) Poumbga, C.; Daniel, C.; Bénéard, M. *J. Am. Chem. Soc.* **1991**, *113*, 1090.

(18) These irreducible representations are  $A_g$  and  $B_{1u}$  respectively for molecules **1–4**, which belong to the  $D_{2h}$  point group, and A and B for **5**, which belongs to the  $C_2$  point group. In this latter case, it was necessary to truncate the virtual space according to the slightly more complex procedure detailed in ref 17e.

(19) The computed S-T splitting at the experimental geometry ( $d_{\text{Zr-Zr}} = 3.653$  Å) is 10 065 cm<sup>-1</sup>. We previously reported a S-T splitting of 8500 cm<sup>-1</sup> for the experimental conformation of this molecule.<sup>8</sup> The larger value obtained in the present work should be attributed to the contribution of the extra, diffuse GTO (exponent 0.045; density maximum at 3.06 Å) that has been added to the valence d shell.

(20)  $d_{\text{Ti-Ti}} = 3.943/3.968$  Å for  $[\text{Cp}_2\text{Ti}(\mu\text{-Cl})_2]$ ;<sup>10</sup> 3.926 Å for  $[(\text{MeCp})_2\text{Ti}(\mu\text{-Cl})_2]$ ;<sup>10</sup> 4.125 Å for  $[(\text{MeCp})_2\text{Ti}(\mu\text{-Br})_2]$ ;<sup>10</sup> 3.918 Å for  $[\text{Cp}_2\text{Ti}(\mu\text{-PMe}_2)_2]$ .<sup>21</sup> Rather unexpectedly, the replacement of  $\text{PMe}_2$  by  $\text{PEt}_2$  bridging ligands reduces the Ti...Ti distance from 3.918 to 3.719 Å,<sup>5b</sup> illustrating the high sensitivity of the metallacycle conformation to steric environment.

(21) Payne, R.; Hachgenei, J.; Fritz, G.; Fenske, D. *Z. Naturforsch.* **1986**, *41b*, 1535.

(22)  $\text{Zr}_2\text{Cl}_6(\text{dppe})_2$ ,  $d_{\text{Zr-Zr}} = 3.099/3.109$  Å;<sup>3</sup>  $\text{Zr}_2\text{Cl}_6(\text{PET}_3)_4$ ,  $d_{\text{Zr-Zr}} = 3.169$  Å;<sup>3</sup>  $\text{Zr}_2\text{Cl}_6(\text{PMe}_2\text{Ph})_4$ ,  $d_{\text{Zr-Zr}} = 3.127$  Å;<sup>3</sup>  $\text{Zr}_2\text{Cl}_6(\text{PBu}_3)_4$ ,  $d_{\text{Zr-Zr}} = 3.182$  Å.<sup>1</sup>

(23)  $(\eta^5\text{-}\eta^5\text{-C}_{10}\text{H}_8)[(\eta^5\text{-C}_5\text{H}_5)\text{Zr}(\mu\text{-Cl})_2]$ ,  $d_{\text{Zr-Zr}} = 3.233$  Å;<sup>2c</sup>  $(\eta^5\text{-}\eta^5\text{-C}_{10}\text{H}_8)[\text{CpZr}(\mu\text{-SPh})_2]$ ,  $d_{\text{Zr-Zr}} = 3.420$  Å.<sup>4d</sup> Another class of Zr(III) dimers with long metal-metal bonds should gather the complexes with little steric strain originating in the peripheral ligands, but accommodating large bridging atoms such as iodine. The order of magnitude of the Zr-Zr bond length is then 3.4–3.5 Å:  $\text{Zr}_2\text{I}_6(\text{PMe}_3)_4$ , 3.393 Å;<sup>7</sup>  $\text{Zr}_2\text{I}_6(\text{PMe}_2\text{Ph})_4$ , 3.439 Å;<sup>7</sup>  $\text{C}_{10}\text{H}_8[\text{CpZr}(\mu\text{-I})_2]$ , 3.472 Å.<sup>4c</sup>

orbitals still increases the electron repulsion in that region. In order to avoid this destabilizing repulsion, the metal  $d_{z^2}$  orbital is progressively depopulated as the M–M distance increases to the benefit of the  $d_{x^2-y^2}$  orbital. The  $\sigma$  character is rapidly vanishing in the bridged Ti(III) dimers which end up at large Ti–Ti distances with nonoverlapping  $d_{z^2-x^2}$  orbitals. In bridged Zr(III) dimers, the evolution is much more smooth and the HOMO presents between 3.6 and 4.0 Å the character of a  $d_{z^2-y^2}$  orbital retaining an important  $\sigma$  character. When the bridging ligands are removed as in the  $[\text{Cp}_2\text{Zr}]_2^{2+}$  model complex, the  $\sigma$  overlap is not hindered anymore and the metal orbitals retain their pure  $\sigma$  character even at a large distance, thus generating a stronger overlap and a larger S–T splitting.

The behavior of dimers of Ti(III) is quite different from that of the equivalent complexes of zirconium, as could be deduced from the observed Ti–Ti equilibrium distances, consistently longer than in the dimers of Zr(III).<sup>20</sup> The reported antiferromagnetism of  $[\text{Cp}_2\text{Ti}(\mu\text{-X})]_2$  (X = Cl or Br)<sup>9</sup> and  $[\text{Cp}_2\text{Ti}(\mu\text{-}(\text{PET})_2)]_2$ <sup>5b</sup> is also at variance from the diamagnetism observed in all Zr(III) dimers. Calculations show that a direct, through-space interaction does exist between the titanium atoms, but this coupling is considerably weaker than for Zr(III) dimers and rapidly vanishes when the Ti–Ti distance increases. The computed S–T splitting is 2420  $\text{cm}^{-1}$  at  $d_{\text{Ti-Ti}} = 3.07$  Å and 860  $\text{cm}^{-1}$  at  $d_{\text{Ti-Ti}} = 3.37$  Å, suggesting that a Ti(III) dimer could be diamagnetic in that range of Ti–Ti distances, due to a metal–metal  $\sigma$  bond. Beyond 3.4 Å, one is left with an antiferromagnetic interaction, the value of  $-J$  decreasing as an inverse function of the metal–metal distance. As a matter of fact, an antiferromagnetic coupling has been detected recently in a dimer of Ti(III) with  $d_{\text{Ti-Ti}} = 3.44$  Å.<sup>24</sup> The lowest singlet and triplet states are computed to be degenerate at  $d_{\text{Ti-Ti}} \sim 3.9$  Å, and the triplet becomes the computed ground state at larger distances ( $J = +26$   $\text{cm}^{-1}$  at  $d_{\text{Ti-Ti}} = 4.17$  Å). The quasi-degeneracy of the singlet and triplet states computed for the experimental conformation is slightly at variance from the experimental findings, since an antiferromagnetic coupling ( $J = -111$   $\text{cm}^{-1}$ ) was reported for **2**.<sup>9</sup> This settles the error boundary that can be assigned to our methodology, which is known to provide a better description of high spin states unless a very high level of dynamic correlation can be afforded.<sup>25</sup>

To summarize, the potential energy curves and S–T splittings computed for Zr(III) and Ti(III) dimers strongly suggest the persistence of a Zr–Zr  $\sigma$  bond at metal–metal distances over 3.5 Å, whereas the Ti–Ti bond vanishes into an antiferromagnetic coupling at much shorter distances. The very long metal–metal distances observed for Zr(III) dimers displaying two Cp rings in each metal fragment should be attributed to a compromise between the steric repulsion originating in the Cp rings and the restoring force associated with the metal–metal bond.<sup>26</sup> Because of a more contracted, less polarizable valence d shell, this force is rapidly vanishing in the equivalent titanium dimers, and the two metal atoms are rejected very far apart.<sup>27</sup> This is reminiscent of what is observed in  $d^8$  quadruply bonded dimetal tetracarboxylates, with M = Cr and Mo. In dimolybdenum complexes, the quadruple bond is strong enough to maintain the Mo–Mo distance in a narrow range around 2.13 Å.<sup>28</sup> At variance from that, the Cr–Cr

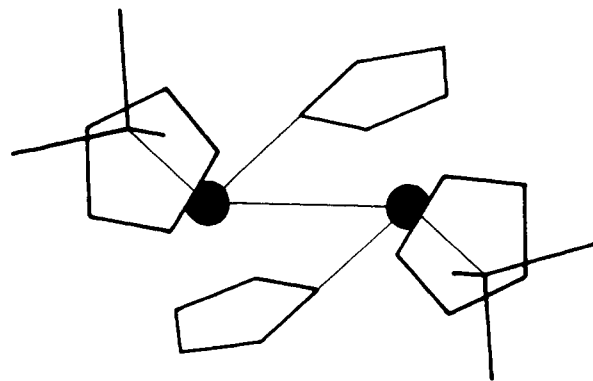


**Figure 5.** The  $[\text{Cp}(\mu\text{-}\eta^1\text{:}\eta^5\text{-C}_5\text{H}_4)\text{Ti}(\text{PMe}_3)]_2$  molecule (**5**) represented in the plane containing the Ti–Ti axis and perpendicular to the  $C_2$  axis.

quadruple bond in tetracarboxylates appears much weaker, possibly at the limit of a multiple antiferromagnetic coupling<sup>29</sup> due to the contraction of the 3d shell and to the consecutive weakness of the d–d overlap.<sup>30</sup> In a similar way, tertiary phosphines of Cr(III) and Mo(III) exhibit long metal–metal bonds and antiferromagnetic behavior whereas a strong metal–metal interaction was found in  $\text{W}_2\text{Cl}_6(\text{PET}_3)_4$ .<sup>27b</sup>

#### 4. The Ti–Ti Coupling in $[\text{Cp}(\mu\text{-}\eta^1\text{:}\eta^5\text{-C}_5\text{H}_4)\text{Ti}(\text{PMe}_3)]_2$ (**5**)

The synthesis and characterization of **5** was reported by Kool et al. in 1986.<sup>11</sup> Each titanium atom is coordinated in an  $\eta^5$  fashion to two cyclopentadienyl rings, one of which is also acting as a two-electron  $\sigma$  donor toward the second metal atom ( $\eta\text{-}\eta^5$  bonding). The molecule belongs to the  $C_2$  symmetry point group. It is represented in Figure 5 in the plane containing the Ti–Ti line ( $z$  axis) and perpendicular to the rotation axis ( $x$  axis). The complex is reported to be diamagnetic, with a Ti–Ti distance of 3.22 Å. The problem of the origin of the diamagnetism, either a Ti–Ti bond or a spin pairing through the bridging  $\text{C}_5\text{H}_4$  cycles, had already been addressed by Kool et al., who concluded in favor of the superexchange mechanism in view of the rather long Ti–Ti distance. Ten years earlier, however, Pez reported the structure of another complex of  $(\text{Ti}_2)^{6+}$ , namely,  $(\eta^5\text{-C}_5\text{H}_5)_2\text{Ti}(\mu\text{-}\eta^1\text{:}\eta^5\text{-C}_5\text{H}_4)\text{Ti}(\eta^5\text{-C}_5\text{H}_5)(\text{C}_4\text{H}_8\text{O})$  with  $d_{\text{Ti-Ti}} = 3.336$  Å, and advocated the presence of “at least a two-electron titanium–titanium linkage”.<sup>31</sup> The question of the existence of a direct metal–metal bond in dinuclear complexes of Ti(III) therefore remains open. The indications given by the singlet–triplet splitting computed for  $[\text{Cp}_2\text{Ti}(\mu\text{-Cl})]_2$  as a function of the Ti–Ti distance are ambiguous: in the considered range of distances (3.2–3.3 Å), the S–T splitting associated with the reported mixture of metal  $d_{z^2}$  and  $d_{x^2-y^2}$   $\sigma$ -type orbitals should reach the order of magnitude of 700–1000  $\text{cm}^{-1}$  (Figure 3). Such a separation should be assimilated to a strong antiferromagnetic coupling and be compatible with the detection of a thermally populated triplet state.<sup>32</sup> The observation of an antiferromagnetic coupling in  $[\text{TiCl}_3(\text{dippe})]_2$ , a chlorine-bridged dimer of Ti(III) with  $d_{\text{Ti-Ti}} = 3.44$  Å, agrees with our results.<sup>24</sup>

We therefore investigated the nature of the diamagnetic coupling and the S–T energy separation in **5** using the same methodology as for molecules **1–4**. As for those molecules, a qualitative explanation of the geometric and electronic structures of complex **5** should refer to the theoretical treatment of  $\text{Cp}_2\text{ML}_n$  complexes by Lauher and Hoffmann.<sup>33</sup> The bending of a  $\text{MCp}_2$  fragment

(24) Hermes, A. R.; Girolami, G. S. *Inorg. Chem.* **1990**, *29*, 313.

(25) Rawlings, D. C.; Gouterman, M.; Davidson, E. R.; Feller, D. *Int. J. Quantum Chem.* **1985**, *28*, 823.

(26) The balance between the steric repulsion of the Cp ligands and the stabilization due to the metal–metal bond should also influence the thermal stability of the  $[\text{Cp}_2\text{Zr}(\mu\text{-X})]_2$  complexes, with X = Cl, Br, or I. Since “small” bridging atoms like chlorine lead to shorter Zr–L bond lengths and therefore favor shorter Zr–Zr distances, by that very fact they enhance both the metal–metal overlap and the Cp–Cp repulsion. Molecules with bigger bridging atoms like Br or I have larger Zr–L bond lengths, which gives the metallacycle more flexibility, through the Zr–X–Zr angle, to adjust to those opposite effects. The strain in the halogen-bridged Zr(III) dimers therefore decreases as the Zr–X distance increases, in agreement with the observed trend in the thermal stabilities of those complexes, varying as  $\text{I} > \text{Br} > \text{Cl}$ .<sup>4b</sup>

(27) (a) Cotton, F. A. *Polyhedron* **1987**, *6*, 667. (b) Cotton, F. A.; Eglin, J. L.; Luck, R. L.; Son, K. *Inorg. Chem.* **1990**, *29*, 1802.

(28) Cotton, F. A.; Walton, R. A. *Multiple Bonds Between Metal Atoms*; John Wiley & Sons: New York, 1988.

(29) See for instance: Corrêa de Mello, P.; Edwards, W. D.; Zerner, M. *C. J. Am. Chem. Soc.* **1982**, *104*, 1440; *Int. J. Quantum Chem.* **1983**, *23*, 425.

(30) (a) Troglor, W. C. *J. Chem. Ed.* **1980**, *57*, 424. (b) Calais, J. L.; Delhalle, J. In *Understanding Molecular Properties*; Avery, J., Dahl, J. P., Hansen, A. E., Eds.; D. Reidel: Dordrecht, 1987; pp 511–519. (c) Wiest, R.; Strich, A.; Bénard, M. *New J. Chem.* **1991**, *15*, 801.

(31) Pez, G. P. *J. Am. Chem. Soc.* **1976**, *98*, 8072.

(32) Bachmann, B.; Hahn, F.; Heck, J.; Wunsch, M. *Organometallics* **1989**, *8*, 2523.

(33) (a) Lauher, J. W.; Hoffmann, R. *J. Am. Chem. Soc.* **1976**, *98*, 1729. (b) Albright, T. A.; Burdett, J. K.; Whangbo, M. H. *Orbital Interactions in Chemistry*; Wiley-Interscience: New York, 1984; pp 394–401.

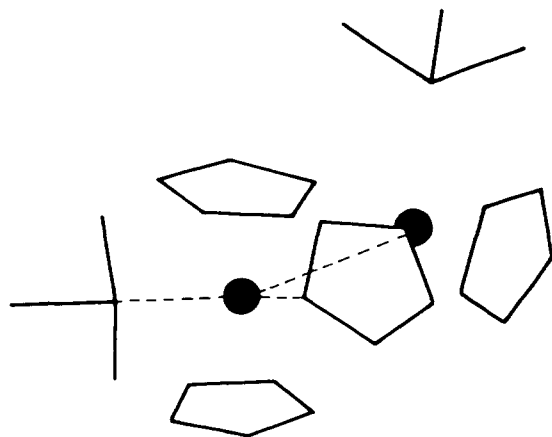


**Figure 6.** Representation of **5** in a plane perpendicular to the bisector plane of the two Cp rings in the  $\eta^5$  position with respect to Ti(1).

generates three hybrid orbitals in the plane containing the metal and bisecting the planes of the two  $\eta^5$ -Cp rings.<sup>33</sup> With one electron left on the metal, the  $\text{Ti}^{\text{III}}\text{Cp}_2$  fragment can therefore accommodate the  $\sigma$ -donor ligands  $\text{PMe}_3$  and  $\eta^1\text{-C}_5\text{H}_4$ , while the third hybrid remains available for a  $\sigma$  coupling with the second Ti(III) fragment. As noted by Lauher and Hoffmann,<sup>33</sup> the L substituents are forced to lie in the mirror plane bisecting the planes of the two Cp rings. Those bisector planes are not easy to visualize in complex **5** since there are not in this case even local elements of symmetry. Figure 6 should be illustrative in conceiving the electronic structure of the dimer in terms of Lauher and Hoffmann's model, since the molecule is projected in a plane perpendicular to the bisector plane of one  $\text{TiCp}_2$  moiety. As in a standard  $\text{Cp}_2\text{ML}_3$  molecule, the three L ligands, namely,  $\text{PMe}_3$  (left), the  $\sigma$ -donor carbon of  $\eta^1\text{-C}_5\text{H}_4$  (center), and the second titanium atom (right), approximately lie in the bisector plane of  $\text{Ti}(\text{I})\text{Cp}_2$ , perpendicular to the plane of projection.<sup>34</sup> The deviation from planarity is almost negligible for  $\text{PMe}_3$  (0.15 Å) and for the  $\eta^1$ -carbon (0.02 Å). It is more important for the second metal atom (1.16 Å, Figure 6), due to the constraints of the  $\eta$  coordination with  $\text{C}_5\text{H}_4$ . As a consequence, the third hybrid of Ti(1) is not exactly pointing toward the corresponding orbital of the other metal fragment. The direction of both singly occupied hybrids deviates by  $21^\circ$  from the Ti-Ti line, thus generating a *bent metal-metal bond* (Figure 7a). This bent bond is described by the HOMO of the SCF wave function with a metal weight of 85%. Some contribution from the  $\text{C}_5\text{H}_4$  cycles (10%) arises from slight destabilizing four-electron interactions between the metal hybrid combination and the orbitals accommodating the  $\sigma$  electrons of the cycles. The LUMO represents the exact antibonding counterpart of the HOMO. The HOMO and the LUMO remain practically unmodified in the set of natural orbitals obtained from the CI calculation with respective populations of 1.54 e and 0.43 e. They are both represented in Figure 7 in terms of electron density.

The populations of the  $\sigma$  and  $\sigma^*$  natural orbitals suggest that the delocalization of the metal electrons is more important for **5** than for  $[\text{Cp}_2\text{Ti}(\mu\text{-Cl})]_2$  in the same range of metal-metal distances (Figure 4). The computed S-T splitting,  $4607\text{ cm}^{-1}$ , confirms that we are faced here with a stronger Ti-Ti bond. The relative strength of the metal-metal bond and the increase of the S-T splitting should not be attributed to an expansion in space of the 3d orbital lobes: the relative contributions of the four CGTOs describing the 3d orbitals are similar for  $[\text{Cp}_2\text{Ti}(\mu\text{-Cl})]_2$  at  $d_{\text{Ti-Ti}} = 3.37\text{ Å}$  and for **5**. The origin of the strong  $\sigma$  bond in **5** lies in a more efficient directionality of the metal hybrids, in spite of the bond bending, resulting in a better Ti-Ti overlap. It

(34) In that sense, the electronic structure of **5** is not basically different from that of the  $[\text{Cp}_2\text{M}(\mu\text{-X})]_2$  symmetric molecules investigated in the first part of this work. What makes **5** more difficult to visualize as a  $\text{Cp}_2\text{ML}_3$  dimer is the metal-metal coupling occurring from the overlap of the *lateral* hybrids, and not of the central ones.

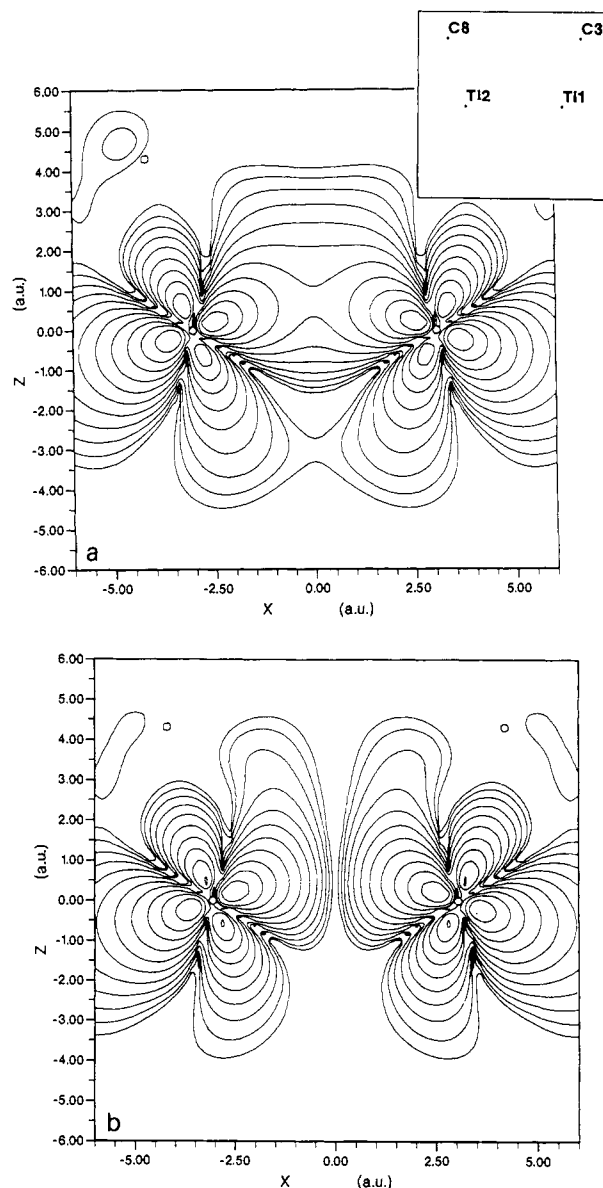


**Figure 7.** Plot of the density generated by the  $\sigma$ (a) and  $\sigma^*$ (b) natural orbitals of **5**. Each orbital is assumed to be populated with two electrons. The outermost contour corresponds to a density of  $0.001\text{ e}\cdot\text{Å}^{-3}$ , and the density is doubled at each subsequent contour.

has been noted that, in the  $[\text{Cp}_2\text{M}(\mu\text{-X})]_2$  complexes, the metal-metal overlap could be hindered by the accumulation of non-bonding electron density arising from the  $\sigma$  lone pairs of the bridging ligands. Since the metal-metal coupling occurs in **5** through the overlap of lateral (and not central)<sup>34</sup> hybrids of the  $\text{Cp}_2\text{M}$  moieties, such an interference with the ligand orbitals should be excluded. The result is an amplification of the overlap and electron delocalization between the titanium atoms, eventually leading to an increase of the S-T splitting. A similar effect has been noticed above for the unsupported metal dimer  $(\text{Cp}_2\text{Zr})_2^{2+}$  as compared to  $[\text{Cp}_2\text{Zr}(\mu\text{-PH}_2)]_2$ . The same efficiency in hybridization occurs in complex **5** as evidenced by the small density contribution in the direction perpendicular to the bent bond (Figure 7).

## 5. Conclusion and Summary

Roald Hoffmann et al. have noticed that "in the case of bridged, supported metal centers the nagging doubt always remains as to the nature of the forces holding the two metals a certain distance apart and making for a low-spin ground state configuration".<sup>35</sup>

(35) Jemmis, E. D.; Pinhas, A. R.; Hoffmann, R. *J. Am. Chem. Soc.* **1980**, *102*, 2576.

In spite of the inescapable tangle between the metal-metal and the metal-ligand-metal contributions to the stability of bridged dimers, the existence of very long bonds in some Zr(III) dimers has been suggested recently by several experimental<sup>5-7</sup> and theoretical<sup>7,8</sup> investigations. The present ab initio calculations provide evidence that the bond lengths observed in  $[\text{Cp}_2\text{Zr}(\mu\text{-X})_2]$  dimers and the reported diamagnetism of those molecules can be explained only by such "superlong" metal-metal  $\sigma$  bonds. The abnormally large Zr-Zr bond lengths are explained by the existence of steric repulsions that develop between the cyclopentadienyl ligands in the cis position with respect to the dimetal unit. This repulsion had been estimated previously by means of SCF calculations to reach 6 kcal·mol<sup>-1</sup> for  $[(\text{C}_5\text{H}_5)_2\text{Zr}(\mu\text{-PH}_2)]_2$  at the observed geometry ( $d_{\text{Zr-Zr}} = 3.65 \text{ \AA}$ ).<sup>8</sup> Since the Zr-Zr  $\sigma$  bond is expected to act as a restoring force balancing the steric repulsion, this value of 6 kcal·mol<sup>-1</sup> could therefore fix an order of magnitude to the stabilization energy attributable to the "superlong" Zr-Zr bond. The comparable structures<sup>7,36</sup> and the diamagnetism of Hf(III) dinuclear complexes<sup>36</sup> suggest that a similar rationalization should hold for those dimers. In contrast to that, the 3d orbitals of titanium, more contracted and less polarizable, cannot overlap enough to balance the steric repulsion of the opposite Cp rings. The metal-metal distances then become larger than 3.7 Å, and the Ti-Ti interaction is reduced to an antiferromagnetic coupling.

(36) (a) Cotton, F. A.; Kibala, P. A.; Wojtczak, W. A. *Inorg. Chim. Acta* 1990, 177, 1. (b) Girolami, G. S.; Wilson, S. R.; Morse, P. M. *Inorg. Chem.* 1990, 29, 3200.

The weakening of the metal-metal  $\sigma$  overlap when the metallacycle flattens finds another origin in the region of nonbonding charge concentration generated around the center of symmetry of the system by the close contact of the bridging ligand lone pairs. The presence of this charge density generates a repulsive interaction with the metal-metal bonding combination of  $d_{z^2}$  orbitals, which responds by progressively transforming into a nonbonding  $d_{xz}$  combination. In the considered range of distances (3.0-4.0 Å) this rehybridization is slow and partial for Zr(III) dimers, which retain significant  $\sigma$  character up to  $d_{\text{Zr-Zr}} = 4 \text{ \AA}$ . Conversely, the transformation into  $d_{z^2}$  orbitals is already complete for bridged Ti(III) dimers at  $d_{\text{Ti-Ti}} = 3.65 \text{ \AA}$ .

As for the  $[\text{Cp}_2\text{Ti}(\mu\text{-X})_2]$  complexes, the electronic structure of  $[\text{Cp}(\mu\text{-}\eta^1\text{:}\eta^5\text{-C}_5\text{H}_4)\text{Ti}(\text{PMe}_3)]_2$ , belonging to the  $C_2$  point group, can be rationalized in terms of coupled  $\text{Cp}_2\text{ML}_3$  fragments. At variance from the  $C_{2v}$  complexes, however, no steric repulsion develops between the Cp cycles, and the metal-metal  $\sigma$  coupling occurs through the overlap of lateral hybrid orbitals of the  $\text{Cp}_2\text{Ti}$  fragments. A relatively short metal-metal distance (3.223 Å) can therefore be observed, and the Ti-Ti  $\sigma$  overlap is not hindered by charge concentrations arising from the other ligands. A rather strong Ti-Ti  $\sigma$  bond is then obtained in spite of the slight tilt angle (21°) of the overlapping metal orbitals.

**Acknowledgment.** All calculations have been carried out on the CRAY-2 computer of the CCVR (Palaiseau, France) through a grant of computer time from the Conseil Scientifique du Centre de Calcul Vectoriel pour la Recherche.

## Geometry Optimization through Second-Moment Scaling

L. M. Hoistad, S. Lee,\* and J. Pasternak

Contribution from the Department of Chemistry, University of Michigan, 930 North University Avenue, Ann Arbor, Michigan 48109-1055. Received November 22, 1991

**Abstract:** We show that second-moment-scaled Hückel theory can be used to account for the bond length variations found in elemental gallium, borohydride, transition metal carbonyl, and hydrocarbon structures. Among the systems investigated are Ga,  $\text{B}_8\text{H}_8^{2-}$ ,  $\text{B}_9\text{H}_9^{2-}$ ,  $\text{B}_{10}\text{H}_{10}^{2-}$ ,  $\text{Os}_5(\text{CO})_{16}$ ,  $\text{Ir}_4(\text{CO})_{12}$ ,  $[\text{Re}_4(\text{CO})_{16}]^{2-}$ , buckminsterfullerene, naphthalene, spiropentane, and butadiene. We also show that the second-moment-scaled Hückel theory correctly resolves the differences in energies among the closo, nido, and arachno borohydride cluster forms. These latter results are in good agreement with Wade's rules for clusters. Finally, we discuss the underlying assumptions of second-moment-scaled theory.

Much of our understanding of the variations in bond distances comes from extended Hückel (eH) molecular orbital calculations and overlap population analyses. This latter technique has been successfully applied to the full range of chemical compounds including main group, transition metal, molecular, and solid-state systems. The overlap population method and its applications have been well reviewed.<sup>1</sup> Briefly, in this method one holds all bonds of a given type (e.g., C-C or B-B bonds) at the same single length. One then calculates the net amount of in-phase or out-of-phase atomic overlap in all the occupied molecular orbitals for a specific pair of atoms. This net amount of overlap is the overlap population.<sup>2</sup> It is found that this overlap population correlates well with the actual bond distances.

This technique however has a shortcoming in that one cannot in general deduce quantitatively the variations in bond lengths.<sup>3</sup> In part, the reason for this is the difficulty one has of studying directly changes in bond lengths with Hückel molecular orbital calculations. Indeed, it is for this reason that one holds bond length constant in deriving useful overlap populations.

Recently, a new modification of Hückel molecular orbital theory has been introduced which obviates the need for careful adjustment of bond lengths.<sup>4</sup> This modification, which we call second-moment scaling, has been proven successful in rationalizing crystalline structure type as a function of electron count for a variety of

(1) Discussions of the overlap population method are given in: (a) Albright, T. A.; Burdett, J. K.; Whangbo, M.-H. *Orbital Interactions in Chemistry*; Wiley: New York, 1985; p 21. (b) Salem, L. *The Molecular Orbital Theory of Conjugated Systems*; Benjamin: New York, 1966; p 134.

(2) The formal definition for overlap population between two atomic orbitals  $\Phi_\mu$  and  $\Phi_\nu$  is  $P_{\mu\nu} = \sum_i 2N_i C_{\mu i} C_{\nu i} S_{\mu\nu}$ , where  $N_i$  is the occupation of the  $i$ th molecular orbital,  $S_{\mu\nu}$  is the overlap integral between  $\Phi_\mu$  and  $\Phi_\nu$ , and  $C_{\mu i}$  and  $C_{\nu i}$  are the LCAO coefficients for the  $i$ th molecular orbital.

(3) It should be noted that in the case of unsaturated hydrocarbons one can find a quantitative relation between overlap population and bond lengths. See: Coulson, C. A.; Golebiewski. *Proc. Phys. Soc., London* 1961, 78, 1310.

(4) Early applications of the second moment scaling hypothesis are given in: (a) Pettifor, D. G.; Podloucky, R. *Phys. Rev. Lett.* 1984, 53, 1080. (b) Burdett, J. K.; Lee, S. J. *Am. Chem. Soc.* 1985, 107, 3063. More recent work: (c) Cressoni, J. C.; Pettifor, D. G. *J. Phys.: Condens. Matter*, submitted for publication. (d) Lee, S. J. *Am. Chem. Soc.* 1991, 113, 101. (e) Lee, S. J. *Am. Chem. Soc.* 1991, 113, 8216. (f) Hoistad, L. M.; Lee, S. J. *Am. Chem. Soc.* 1991, 113, 8216. (g) Lee, S. *Acc. Chem. Res.* 1991, 24, 249.

\* Author to whom correspondence should be addressed.